Organic LETTERS

Letter

pubs.acs.org/OrgLett

The CH−π Interactions of Methyl Ethers as a Model for Carbohydrate−*N*-Heteroarene Interactions

Ping Li,[†] Trent M. Parker,[‡] Jungwun Hwang,[†] Fengyuan Deng,[†] Mark D. Smith,[†] Perry J. Pellechia,[†] C. David Sherrill,[‡] and Ken D. Shimizu*[,†]

[†]Department of Chemistry and Biochemistry, University of South Carolina, Columbia, South Carolina 29208, United States

[‡]Center for Computational Molecular Science and Technology, School of Chemistry and Biochemistry and School of Computational Science and Engineering, Georgia Institute of Technology, Atlanta, Georgia 30332, United States

Supporting Information

ABSTRACT: CH−π interactions have been cited as an important contributor to carbohydrate recognition. To determine whether *N*-heterocycles form stronger CH−π interactions, the interactions of methyl ether groups with heterocyclic and nonheterocyclic aromatic surfaces were studied. Both experimental and computational experiments found that *N*-heterocyclic aromatic surfaces formed stronger interactions. This enhancement was attributed to attractive dipole−dipole interactions between the methyl ether C−O bond and the *N*-heterocyclic aromatic dipole.

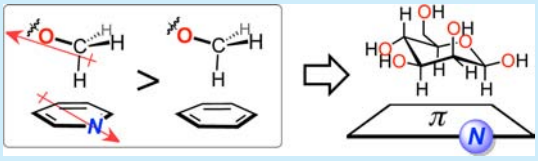

Carbohydrate recognition plays a key role in many biological processes[1] such as fertilization,[2] immune response,[3] and inflammation.[4] Thus, the study of factors that enhance carbohydrate affinity and selectivity has been the focus of extensive research efforts.[5] While hydrogen bonding is generally considered the primary interaction,[6] CH−π interactions[7] have also been cited as key contributors to carbohydrate binding.[8] Interestingly, a high percentage of the CH−π interactions of carbohydrates involve heterocyclic aromatic surfaces.[9] For example, the protein−sugar complex between *Urtica dioica* agglutinin and the triose NAG3 contains four CH−π interactions each involving a different heterocyclic aromatic residue (Trp21, Trp23, His67, and Trp69) (Figure 1a).[10] Thus, the goal of this work was to determine whether carbohydrates form stronger CH−π interactions with heterocyclic versus nonheterocyclic aromatic surfaces. Our strategy was to employ a small molecule model system in conjunction with computational studies to address this question. In this study, methyl ether groups were used as minimalistic models of carbohydrates. Methyl ethers can form similar CH−π interactions as those in carbohydrates, as they have alkyl groups directly attached to polar oxygens (Figure 1b). In addition, the methyl ether groups lack hydrogen bond donating OH groups that would complicate the analysis. We found that the presence of the ether oxygen plays a key role in modulating the interaction energies and geometries of this moiety.

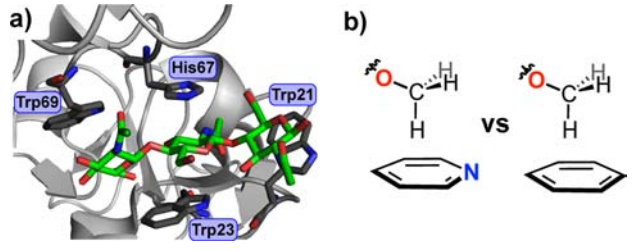

Figure 1. (a) Crystal structure of the active site of the *Urtica dioica* agglutinin with a bound tri-*N*-acetylchitotriose (NAG3).[10] The heterocyclic residues that form CH−π interactions (Trp69, Trp23, His67, and Trp21) are highlighted (PDB entry 1EHH). (b) Schematic representation of the CH−π interactions of a methyl ether group with an *N*-heterocyclic and nonheterocyclic aromatic ring.

Molecular torsional balances are small molecule model systems designed to measure the strength of intramolecular noncovalent interactions via shifts in a conformational equilibrium.[11] Utilizing this strategy, we have recently developed a rigid bicyclic molecular balance that has been successfully applied to study a number of weak noncovalent interactions including $\pi-\pi$,[12] CH−π,[13] deuterium−π,[14] and heterocyclic−π interactions.[15] For this study, these balances were modified to study the CH−π interactions of heterocyclic and nonheterocyclic aromatic surfaces (Figure 2). Balances **1**−**6** were designed with a methyl arm (OCH_3 or CH_2CH_3) and an aromatic surface containing two, one, or zero *N*-heterocyclic units that could form an intramolecular CH−π interaction. The balances were synthesized via the same modular route.[12−15]

First, the ability of balances **1**−**6** to form an intramolecular CH−π interaction in the *folded* conformer between the methyl arm and the aromatic shelf was assessed in solution and in the solid state. In solution (CD_2Cl_2), large upfield chemical shifts were observed for the *folded* versus *unfolded* methyl arm protons in the ^{1}H NMR spectra (Table 1). These upfield shifts ($\Delta\delta$ = 1.3 to 1.5 ppm) were consistent with the methyl groups being in contact with the aromatic shelf in the *folded* conformers and forming the desired intramolecular CH−π interactions. The

Received: August 14, 2014
Published: September 19, 2014

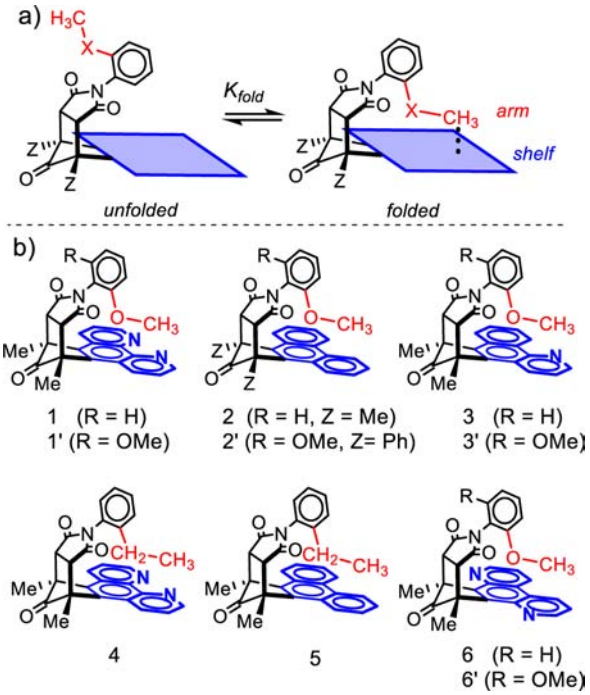

Figure 2. (a) Schematic representation of the *unfolded*–*folded* conformational equilibrium of molecular balances **1**–**3** for measuring the CH–π interactions of the methyl ether group. (b) Structures of the *folded* conformers of molecular balances with methyl ether (**1**, **2**, **3**, and **6**) and with ethyl arms (**4** and **5**) and their two-armed analogues (**1**′, **2**′, **3**′, and **6**′) for X-crystallographic analysis.

Table 1. ^{1}H NMR Solution Measurements of Balances 1–6 in CD_2Cl_2 at 25 °C

balance	CH-π interaction	$\Delta\delta_{CH_3}$ [a]	[folded]/[unfolded] [b]	ΔG [c]
1		1.42	1.04	-0.02
2		1.48	0.59	+0.31
3	 Y = N & CH	1.45	0.79	+0.14
4		1.20	1.33	-0.17
5		1.15	1.41	-0.20
6	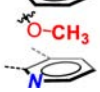	1.31	0.66	+0.25

[a]Difference in ^{1}H chemical shift (ppm) of the CH_3 protons between the *unfolded* and *folded* conformers. [b]Measured from the integration areas of the CH_3 peaks in the ^{1}H NMR spectra (error < ± 5%). [c]Folding energies in kcal/mol (±0.03 kcal/mol).

differences in the chemical shifts of the methyl protons were readily measured at rt, as the *unfolded* and *folded* conformers were in slow exchange in the ^{1}H NMR spectra.[12−15]

The intramolecular CH–π interactions were also characterized in the solid state by X-ray crystallography. To ensure the formation of the *folded* conformers in the solid-state, "two-armed" balances (**1**′, **2**′, **3**′, and **6**′) were prepared and crystallized.[12,13,15] The two-armed balances have the same arm at both *ortho*-positions of the pivot ring; thus, one arm is always in the *folded* conformation, and the other arm is in the *unfolded* conformation. X-ray crystallographic analysis of **1**′–**3**′ and **6**′ showed the expected intramolecular CH–π interactions (Figure 3). In each structure, a proton on the methyl group of the *folded* arm was within the proper atom-to-plane distance (2.56–2.61 Å) to form a CH–π interaction with the aromatic shelf.[16]

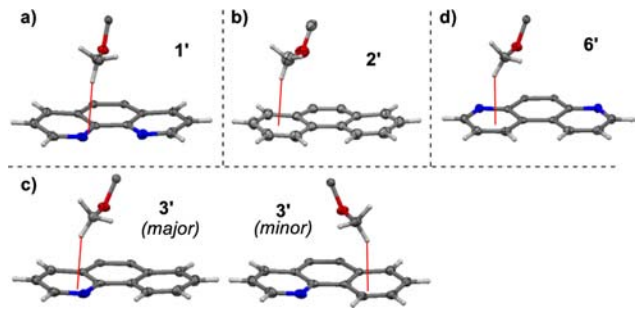

Figure 3. Truncated front views of the X-ray crystal structures of balances **1**′ (a), **2**′ (b), **3**′ (c), and **6**′ (d), highlighting the intramolecular CH–π interactions. In the structure for **3**′, both the **3**′ major and **3**′ minor configurations were observed with a ratio of 62:38. The atom-to-plane distances for the intramolecular CH–π interactions are highlighted as red lines.

Next, the strengths of the CH–π interactions were measured in solution (Table 1). The folding ratios were measured in solution (CD_2Cl_2) by integration of the corresponding peaks in the ^{1}H NMR spectra and converted into folding energies [$\Delta G = -RT\ \ln([folded]/[unfolded])$]. First, the folding energies of balances **1** and **2** were compared to test whether the methyl ether arm formed stronger interactions with heterocyclic or nonheterocyclic aromatic surfaces. Balances **1** and **2** had folding energies of −0.02 and +0.31 kcal/mol, respectively. Thus, the intramolecular interactions in heterocyclic **1** were more stabilizing by −0.33 kcal/mol than in nonheterocyclic **2**. Analysis of hybrid balance **3**, which contained a heterocyclic and a nonheterocyclic ring, provided further evidence that the heterocyclic surface formed stronger intramolecular interactions. The OCH_3 group in **3** can flip back and forth between the heterocyclic and nonheterocyclic outer ring of the benzoquinoline surface.[17] Indeed, both intramolecular CH–π configurations were observed in the crystal structure of **3**′ (Figure 3c). The populations of the two configurations were unequal in the crystal structure, as the OCH_3–heterocyclic interaction was favored by ∼2:1 (62:38). Analyses of the folding ratios of **3** in solution were also consistent with the heterocyclic ring forming stronger intramolecular interactions. The folding energy of **3** (+0.14 kcal/mol) fell almost halfway between the folding energies of the purely heterocyclic and nonheterocyclic balances **1** and **2** (−0.02 and +0.31 kcal/mol).

In assessing the reason for the above stability trends, we arrived at the conclusion that they probably did not arise from differences in the strengths of the CH–π interactions. Our reasoning was that CH–π interactions are generally considered to be dispersion dominated interactions.[18] The dispersion interactions for an *N*-heterocyclic and an isosteric non-

dx.doi.org/10.1021/ol502418k | *Org. Lett.* 2014, 16, 5064–5067

heterocyclic ring should be very similar, as the difference in polarizability of a nitrogen to a CH group is minor.[19] Furthermore, the dipole of the *N*-heterocycle should have little effect on the CH−π interaction. To confirm that heterocyclic and nonheterocyclic surfaces form similar strength CH−π interactions, we conducted *ab initio* calculations (estimated complete-basis-set-coupled-cluster, CCSD(T)/CBS) comparing the CH−π interactions of methane with benzene and pyridine, respectively. Although differences in geometry were observed, the intermolecular interactions in the two systems were isoenergetic (−1.39 versus −1.41 kcal/mol).

Thus, an alternative hypothesis was developed based on the role of the oxygen linkers in balances **1**−**3**. To isolate the influence of the oxygen linker, we synthesized two analogous heterocyclic and nonheterocyclic balances **4** and **5** without oxygen linkers where the OCH_3 groups were replaced by CH_2CH_3 groups. Balances **4** and **5** formed similar intramolecular CH−π interactions as balances **1**−**3**. This was evident from the similarly large upfield chemical shifts (∼1.2 ppm) of their terminal methyl protons in the *folded* conformers (Table 1).

In contrast to methyl ether balances **1**−**3**, balances **4** and **5** had very similar interaction energies for the heterocyclic and nonheterocyclic surfaces. Balances **4** and **5** had folding energies of −0.17 and −0.20 kcal/mol, respectively, which were within experimental error (±0.03 kcal/mol). Thus, both computational and experimental studies concurred that the differences in the interactions between the heterocyclic and nonheterocyclic aromatic surfaces appeared to be due to the oxygen linker.

Two hypotheses were formulated to explain the influence of the oxygen linker on the intramolecular interactions. The first hypothesis was that the oxygen linker was polarizing the C−H bond of the methyl ether. This polarization hypothesis was consistent with theoretical[20] and experimental[21] studies that found that more polarized or acidic C−H bonds form stronger CH−π interactions. The second hypothesis was that the C−O bond dipole was interacting with the heterocyclic dipole. The two hypotheses were tested computationally and experimentally by positioning the OCH_3 group at different angles over the *N*-heterocyclic ring (Figure 4). The dihedral angle (α) of the C−O bond dipole with respect to the heterocycle dipole was systematically varied, and the corresponding interaction energies were measured (Figure 4). For the C−H bond polarization hypothesis, the interaction energy should not vary substantially and would only be weakened when the electronegative O- and N-atoms were in close proximity. However, for the dipole hypothesis, there should be a strong stabilizing as well as a destabilizing effect, depending upon the orientation of the dipoles.

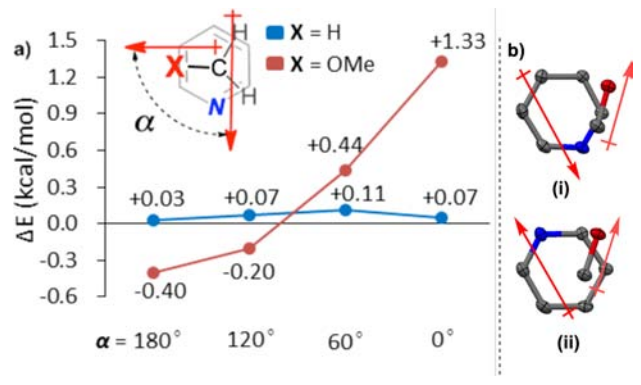

Figure 4. (a) Calculated CCSD(T)/CBS [i.e., MP2/CBS from aug-cc-pVQZ/aug-cc-pV5Z extrapolation + (CCSD(T)/aug-cc-pVTZ − MP2/aug-cc-pVTZ)] interaction energy differences (ΔE) between the heterocyclic and nonheterocyclic CH−π complexes [ΔE = $E(CH_3\mathbf{X}/Py)$ − $E(CH_3\mathbf{X}/Bz)$; **X** = H or OMe] at four different orientations of the dipoles (α = 180°, 120°, 60°, and 0°). (b) Partial top views of the CH−π interaction regions in crystal structures **1**′ (i) and **6**′ (ii) highlighting the orientations of the C−O bond and heterocycle dipoles.

The results from our computational and experimental studies were consistent with the dipole hypothesis. First, the computational study estimated the complexation energy of dimethyl ether with pyridine or benzene. The CH_3 group of dimethyl ether was positioned over the aromatic ring with a single C−H bond forming a CH−π interaction. Intermolecular interaction energies were computed for a series of dihedral angles α. The difference in interaction energies when pyridine was replaced by benzene, ΔE, was plotted as a function of α in Figure 4 (red curve). When the C−O and pyridine dipoles were antiparallel (α = 180°), the interaction between dimethyl ether and pyridine was stabilized compared to the interaction energy between dimethyl ether and benzene (ΔE = −0.40 kcal/mol). When the C−O and pyridine dipoles were parallel (α = 0°), the interaction energy was strongly destabilizing for pyridine versus benzene (ΔE = 1.33 kcal/mol). To confirm that these geometric effects were indeed due to interactions between the C−O dipole and the heterocycle dipole, a control study was performed in which dimethyl ether was replaced in the computations by methane (blue curve in Figure 4). Consistent with our hypothesis, the removal of the C−O dipole by replacing dimethyl ether with methane resulted in very small values for ΔE (the difference between methane/pyridine and methane/benzene) that are nearly constant with respect to α.

A similar experiment was carried out using our molecular balances. The precise positioning of the OCH_3 and heterocycle dipoles was more difficult using a model system. However, we were able to synthesize and test a new balance **6** which had the heterocyclic nitrogens at the 4- and 7-positions. This places the *N*-heterocyclic nitrogens on the opposite edge of the aromatic shelf in comparison to the original 1,10-phenanthroline shelf. Comparison of balances **1** and **6** provided a means to study two different geometries of the interaction. The orientation of the heterocycle dipole of the outer ring on the shelf and the C−O bond from the crystal structures of **1**′ and **6**′ (Figure 4b) most closely correlates to α = 120° and 60°, respectively. Thus, the dipoles in **1** point in opposite directions and the dipoles in **6** point in the same direction. The measured folding energies for **1** and **6** (−0.02 and +0.25 kcal/mol) revealed the same stability trend predicted by the computational study. When the dipoles were antiparallel as in balance **1**, the OCH_3−heterocyclic interaction was more stabilizing (lower in energy). When the dipoles were aligned in the same direction as in **6**, the OCH_3−heterocyclic interaction was destabilized (higher in energy). Symmetry-adapted perturbation theory (SAPT) calculations confirm that this energy variation with orientation is almost entirely electrostatic in nature, consistent with dipole−dipole interactions (see Supporting Information).

In conclusion, we have utilized a combination of theory and model systems to study the CH−π interactions of *N*-heterocyclic and nonheterocyclic surfaces. There was excellent agreement between the two approaches. The $-OCH_3$ group was found to be capable of forming stronger noncovalent interactions with *N*-heterocyclic surfaces. In contrast, the $-CH_2CH_3$ group showed

dx.doi.org/10.1021/ol502418k | *Org. Lett.* 2014, 16, 5064−5067

similar interaction energies for the two types of surfaces. Thus, the methyl ether oxygen appears to play a key role in modifying the interaction energies with heterocyclic surfaces. The O-atom does not appear to enhance the CH−π interaction directly. Instead, the C−O dipole interacts with the heterocycle dipole, which can strengthen or weaken the OCH_3−aromatic interaction. These stability trends may have some bearing on many biologically important carbohydrate−aromatic interactions. The attraction between C−O and heterocycle dipoles explains the prevalence of carbohydrate−heteroarene interactions. This dipole−dipole interaction could also be used to optimize carbohydrate binding in synthetic and bioengineered carbohydrate receptors. New molecular balances containing other biologically relevant heterocyclic motifs, such as tryptophane, pyrimidine, and purines, are currently being developed in our laboratory to further investigate this phenomenon.

■ ASSOCIATED CONTENT

Supporting Information

Experimental details, characterization data for all newly reported compounds, crystal data (cif) for **1′**, **2′**, and **6′**, computational details. This material is available free of charge via the Internet at http://pubs.acs.org.

■ AUTHOR INFORMATION

Corresponding Author

*E-mail: shimizu@mail.chem.sc.edu.

Notes

The authors declare no competing financial interest.

■ ACKNOWLEDGMENTS

This work was supported by the National Science Foundation (NSF) grants CHE 1310139 and CHE 1300497.

■ REFERENCES

(1) (a) Dwek, R. A. *Chem. Rev.* **1996**, *96*, 683. (b) Bertozzi, C. R.; Kiessling, L. L. *Science* **2001**, *291*, 2357. (c) Gabius, H. J.; Siebert, H. C.; Andre, S.; Jimenez-Barbero, J.; Rudiger, H. *ChemBioChem* **2004**, *5*, 740. (d) Garg, H. G.; Cowman, M. K.; Hales, C. A. *Carbohydrate Chemistry, Biology and Medical Applications*, 1st ed.; Elsevier: Amsterdam; Boston, 2008. (e) Walter, F.; Vicens, Q.; Westhof, E. *Curr. Opin. Chem. Biol.* **1999**, *3*, 694. (f) Vicens, Q.; Westhof, E. *ChemBioChem* **2003**, *4*, 1018. (g) Willis, B.; Arya, D. P. *Adv. Carbohydr. Chem. Biochem.* **2006**, *60*, 251. (h) Lis, H.; Sharon, N. *Chem. Rev.* **1998**, *98*, 637.

(2) Benoff, S. *Mol. Hum. Reprod.* **1997**, *3*, 599.

(3) Holmskov, U.; Thiel, S.; Jensenius, J. C. *Annu. Rev. Immunol.* **2003**, *21*, 547.

(4) Lasky, L. A. *Annu. Rev. Biochem.* **1995**, *64*, 113.

(5) (a) James, T. D.; Shinkai, S. Artificial receptors as chemosensors for carbohydrates. In *Topics in Current Chemistry*; Penades, S., Ed.; Springer: Heidelberg, 2002; Vol. *218*, pp 159−200. (b) Striegler, S. *Curr. Org. Chem.* **2003**, *7*, 81. (c) James, T. D.; Phillips, M. D.; Shinkai, S. *Boronic acids in saccharide recognition*; RSC Publishing: Cambridge, 2006. (d) Davis, A. P.; Wareham, R. S. *Angew. Chem., Int. Ed.* **1999**, *38*, 2978. (e) Mazik, M. *Chem. Soc. Rev.* **2009**, *38*, 935. (f) Mazik, M. *RSC Adv.* **2012**, *2*, 2630. (f) Boraston, A. B.; Bolam, D. N.; Gilbert, H. J.; Davies, G. J. *Biochem. J.* **2004**, *382*, 769. (g) Arnaud, J.; Audfray, A.; Imberty, A. *Chem. Soc. Rev.* **2013**, *42*, 4798.

(6) (a) Weis, W. I.; Drickamer, K. *Annu. Rev. Biochem.* **1996**, *65*, 441. (b) Lis, H.; Sharon, N. *Chem. Rev.* **1998**, *98*, 637. (c) Davis, A. P.; Wareham, R. S. *Angew. Chem., Int. Ed.* **1999**, *38*, 2978. (d) Mazik, M. *Chem. Soc. Rev.* **2009**, *38*, 935.

(7) (a) Nishio, M. *Phys. Chem. Chem. Phys.* **2011**, *13*, 13873. (b) Takahashi, O.; Kohno, Y.; Nishio, M. *Chem. Rev.* **2010**, *110*, 6049. (c) Zhang, Z. B.; Xia, B. Y.; Han, C. Y.; Yu, Y. H.; Huang, F. H. *Org. Lett.* **2010**, *12*, 3285. (d) Zhang, Z. B.; Luo, Y.; Chen, J. Z.; Dong, S. Y.; Yu, Y. H.; Ma, Z.; Huang, F. H. *Angew. Chem., Int. Ed.* **2011**, *50*, 1397. (e) Zhang, Z. B.; Yu, G. C.; Han, C. Y.; Liu, J. Y.; Ding, X.; Yu, Y. H.; Huang, F. H. *Org. Lett.* **2011**, *13*, 4818. (f) Xue, M.; Yang, Y.; Chi, X. D.; Zhang, Z. B.; Huang, F. H. *Acc. Chem. Res.* **2012**, *45*, 1294.

(8) (a) Fernandez, M. D.; Canada, F. J.; Jimenez-Barbero, J.; Cuevas, G. *J. Am. Chem. Soc.* **2005**, *127*, 7379. (b) Terraneo, G.; Potenza, D.; Canales, A.; Jimenez-Barbero, J.; Baldridge, K. K.; Bernardi, A. *J. Am. Chem. Soc.* **2007**, *129*, 2890. (c) Laughrey, Z. R.; Kiehna, S. E.; Riemen, A. J.; Waters, M. L. *J. Am. Chem. Soc.* **2008**, *130*, 14625. (d) Ramirez-Gualito, K.; Alonso-Rios, R.; Quiroz-Garcia, B.; Rojas-Aguilar, A.; Diaz, D.; Jimenez-Barbero, J.; Cuevas, G. *J. Am. Chem. Soc.* **2009**, *131*, 18129. (e) Barwell, N. P.; Davis, A. P. *J. Org. Chem.* **2011**, *76*, 6548. (f) Santana, A. G.; Jimenez-Moreno, E.; Gomez, A. M.; Corzana, F.; Gonzalez, C.; Jimenez-Oses, G.; Jimenez-Barbero, J.; Asensio, J. L. *J. Am. Chem. Soc.* **2013**, *135*, 3347. (g) Chen, W. T.; Enck, S.; Price, J. L.; Powers, D. L.; Powers, E. T.; Wong, C. H.; Dyson, H. J.; Kelly, J. W. *J. Am. Chem. Soc.* **2013**, *135*, 9877. (h) Asensio, J. L.; Arda, A.; Canada, F. J.; Jimenez-Barbero, J. *Acc. Chem. Res.* **2013**, *46*, 946. (i) Spiwok, V.; Lipovova, P.; Skalova, T.; Buchtelova, E.; Hasek, J.; Kralova, B. *Carbohydr. Res.* **2004**, *339*, 2275.

(9) (a) Asensio, J. L.; Arda, A.; Canada, F. J.; Jimenez-Barbero, J. *Acc. Chem. Res.* **2013**, *46*, 946. (b) Nishio, M.; Umezawa, Y.; Fantini, J.; Weiss, M. S.; Chakrabarti, P. *Phys. Chem. Chem. Phys.* **2014**, *16*, 12648.

(10) Harata, K.; Muraki, M. *J. Mol. Biol.* **2000**, *297*, 673.

(11) (a) Paliwal, S.; Geib, S.; Wilcox, C. S. *J. Am. Chem. Soc.* **1994**, *116*, 4497. (b) Mati, I. K.; Cockroft, S. L. *Chem. Soc. Rev.* **2010**, *39*, 4195.

(12) Carroll, W. R.; Pellechia, P.; Shimizu, K. D. *Org. Lett.* **2008**, *10*, 3547.

(13) (a) Carroll, W. R.; Zhao, C.; Smith, M. D.; Pellechia, P. J.; Shimizu, K. D. *Org. Lett.* **2011**, *13*, 4320. (b) Zhao, C.; Li, P.; Smith, M. D.; Pellechia, P. J.; Shimizu, K. D. *Org. Lett.* **2014**, *16*, 3520.

(14) Zhao, C.; Parrish, R. M.; Smith, M. D.; Pellechia, P. J.; Sherrill, C. D.; Shimizu, K. D. *J. Am. Chem. Soc.* **2012**, *134*, 14306.

(15) Li, P.; Zhao, C.; Smith, M. D.; Shimizu, K. D. *J. Org. Chem.* **2013**, *78*, 5303.

(16) Nishio, M.; Umezawa, Y.; Honda, K.; Tsuboyama, S.; Suezawa, H. *CrystEngComm* **2009**, *11*, 1757.

(17) Nijamudheen, A.; Jose, D.; Shine, A.; Datta, A. *J. Phys. Chem. Lett.* **2012**, *3*, 1493.

(18) (a) Tsuzuki, S.; Honda, K.; Uchimaru, T.; Mikami, M.; Tanabe, K. *J. Am. Chem. Soc.* **2000**, *122*, 3746. (b) Shibasaki, K.; Fujii, A.; Mikami, N.; Tsuzuki, S. *J. Phys. Chem. A* **2006**, *110*, 4397. (c) Tsuzuki, S.; Honda, K.; Uchimaru, T.; Mikami, M.; Fujii, A. *J. Phys. Chem. A* **2006**, *110*, 10163. (d) Morita, S.; Fujii, A.; Mikami, N.; Tsuzuki, S. *J. Phys. Chem. A* **2006**, *110*, 10583. (e) Tsuzuki, S.; Honda, K.; Fujii, A.; Uchimaru, T.; Mikami, M. *Phys. Chem. Chem. Phys.* **2008**, *10*, 2860. (f) Tsuzuki, S.; Fujii, A. *Phys. Chem. Chem. Phys.* **2008**, *10*, 2584. (g) Fujii, A.; Hayashi, H.; Park, J. W.; Kazama, T.; Mikami, N.; Tsuzuki, S. *Phys. Chem. Chem. Phys.* **2011**, *13*, 14131. (h) Fujii, A.; Hayashi, H.; Tsuzuki, S. *Chem. Phys. Lett.* **2012**, *537*, 11.

(19) (a) Hunter, C. A. *Angew. Chem., Int. Ed.* **2004**, *43*, 5310. (b) Sherrill, C. D. *Acc. Chem. Res.* **2013**, *46*, 1020.

(20) (a) Ugozzoli, F.; Arduini, A.; Massera, C.; Pochini, A.; Secchi, A. *New J. Chem.* **2002**, *26*, 1718. (b) Ribas, J.; Cubero, E.; Luque, F. J.; Orozco, M. *J. Org. Chem.* **2002**, *67*, 7057. (c) Takahashi, O.; Kohno, Y.; Saito, K. *Chem. Phys. Lett.* **2003**, *378*, 509. (d) Amicangelo, J. C.; Gung, B. W.; Irwin, D. G.; Romano, N. C. *Phys. Chem. Chem. Phys.* **2008**, *10*, 2695. (e) Gung, B. W.; Emenike, B. U.; Lewis, M.; Kirschbaum, K. *Chem—Eur. J.* **2010**, *16*, 12357.

(21) (a) Thomas, K. M.; Naduthambi, D.; Zondlo, N. J. *J. Am. Chem. Soc.* **2006**, *128*, 2216. (b) Pandey, A. K.; Naduthambi, D.; Thomas, K. M.; Zondlo, N. J. *J. Am. Chem. Soc.* **2013**, *135*, 4333. (c) Zondlo, N. J. *Acc. Chem. Res.* **2013**, *46*, 1039.